

# Supporting Information

Burman et al. 10.1073/pnas.1120688109

## SI Materials and Methods

**Fly Stocks Used.** The *UAS-CD8GFP*, *UAS-MitoGFP*, *UAS-GFP*, *TH-GAL4*, *Cha-GAL4*, *Repo-GAL4*, and *Elav-GAL4* transgenic lines were obtained from the Bloomington Drosophila Stock Center. The *UAS-MfnRNAi* transgenic line was obtained from the Vienna Drosophila RNAi Center. The ParkinC2 transgenic line was generated in-house. The *park<sup>25</sup>*-null allele (1), *PINK1<sup>B9</sup>* null allele (2), the *UAS-ATG8a* (3), *UAS-Drp1* (4), and *UAS-PINK1* (2) transgenic lines have been described previously.

For Fig. 1 B–D: *w<sup>1118</sup>* = GFP<sup>-</sup>; *UAS-CD8GFP<sup>+/+</sup>*; *TH-GAL4<sup>+/+</sup>* or *UAS-GFP<sup>+/+</sup>*; *TH-GAL4<sup>+/+</sup>* = dopaminergic (DA)-GFP; *UAS-GFP*, *Cha-GAL4<sup>+/+</sup>* = cholinergic (CH)-GFP; *UAS-CD8GFP*, *Elav-GAL4<sup>+/+</sup>* or *Y* = pan-neuronal GFP; *UAS-CD8GFP*, *Repo-GAL4<sup>+/+</sup>* = Glial-GFP.

For Fig. 1E: *UAS-CD8GFP<sup>+/+</sup>*; *TH-GAL4<sup>+/+</sup>* = DA neurons; *UAS-GFP*, *Cha-GAL4<sup>+/+</sup>* = CH neurons.

For Fig. S1A: *UAS-CD8GFP<sup>+/+</sup>*; *TH-GAL4<sup>+/+</sup>* = DA neurons.

For Fig. S1C: *UAS-GFP<sup>+/+</sup>*; *TH-GAL4<sup>+/+</sup>* and *UAS-CD8GFP<sup>+/+</sup>*; *TH-GAL4* and *UAS-mitoGFP<sup>+/+</sup>*; *TH-GAL4<sup>+/+</sup>* = DA neurons.

For Fig. 2A: *UAS-mitoGFP/UAS-CD8GFP* or *UAS-GFP*; *park<sup>25</sup>-THGAL4/park<sup>25</sup>*, *UAS-mitoGFP* or *MKRS* = sibling control and parkin mutant DA neurons.

For Fig. 2B: *UAS-CD8GFP/CyO* or *UAS-PINK1*; *TH-GAL4<sup>+/+</sup>* = sibling control and *PINK1* overexpressing DA neurons.

For Fig. 2C: *UAS-GFP*, *Cha-GAL4/CyO*; *park<sup>25</sup>/MKRS* or *park<sup>25</sup>* = sibling control and parkin mutant CH neurons.

For Fig. 2D: *UAS-GFP*, *Cha-GAL4/CyO* or *UAS-PINK1* = sibling control and *PINK1* overexpressing CH neurons.

For Fig. 2E: Genotypes described above with addition of *PINK1<sup>iva</sup>/Y*; *UAS-CD8GFP<sup>+/+</sup>*; *THGAL4<sup>+/+</sup>*; and *PINK1<sup>B9</sup>/Y*; *UAS-CD8GFP<sup>+/+</sup>*; *THGAL4<sup>+/+</sup>* = *PINK1* control and null mutant DA neurons, respectively; *UAS-CD8GFP/UAS-Parkin<sup>C2</sup>*; *park<sup>25</sup>-THGAL4/park<sup>25</sup>* = *Parkin* overexpression in parkin mutant DA neurons.

For Fig. S2: *UAS-CD8GFP/UAS-CD8GFP*; *TH-GAL4/TH-GAL4* = DA neurons.

For Fig. 3: *UAS-mitoGFP* or *UAS-CD8GFP/CyO*; *park<sup>25</sup>-THGAL4/MKRS* = sibling control; *UAS-mitoGFP* or *UAS-CD8GFP/CyO*; *park<sup>25</sup>/park<sup>25</sup>-THGAL4* = parkin-null; *UAS-mitoGFP/CyO*; *park<sup>25</sup>*, *UAS-Drp1/park<sup>25</sup>*, *THGAL4* = parkin mutant expressing *DRP1*; *UAS-mitoGFP/CyO*; *park<sup>25</sup>*, *UAS-MfnRNAi/park<sup>25</sup>*, *THGAL4* = parkin mutant expressing *MfnRNAi*; *UAS-mitoGFP* or *UAS-CD8GFP/UAS-ATG8a*, *UAS-GFP*; *park<sup>25</sup>/park<sup>25</sup>*, *TH-GAL4* = parkin mutant expressing *ATG8a*. All expression restricted to DA neurons.

For Fig. S3: *UAS-mitoGFP* or *UAS-CD8GFP/CyO*; *park<sup>25</sup>-THGAL4/MKRS* = DA parkin sibling control; *UAS-mitoGFP* or *UAS-CD8GFP/CyO*; *park<sup>25</sup>/park<sup>25</sup>-THGAL4* = DA parkin mutant; *UAS-CD8-GFP<sup>+/+</sup>*; *TH-GAL4<sup>+/+</sup>* = wild-type.

For Fig. 4: CantonS and *w<sup>1118</sup>* = WT; +/CyO; *park<sup>25</sup>/park<sup>25</sup>*, *TH-GAL4* = parkin mutant; +/CyO; *park<sup>25</sup>*, *UAS-Drp1/park<sup>25</sup>*, *TH-GAL4* = parkin mutant expressing *DRP1*; +/CyO; *UAS-MfnRNAi*, *park<sup>25</sup>/park<sup>25</sup>*, *TH-GAL4* = parkin mutant expressing *MfnRNAi*; *UAS-ATG8a*, *UAS-GFP/UAS-*

*mito-GFP*; *park<sup>25</sup>/park<sup>25</sup>-TH-GAL4* = parkin mutants expressing *ATG8a*. All expression restricted to DA neurons.

For Fig. S4A: *UAS-mitoGFP/UAS-CD8GFP* or *UAS-GFP*; *park<sup>25</sup>*, *THGAL4/park<sup>25</sup>*, *UAS-mito-GFP* or *MKRS* = sibling control and parkin mutant DA neurons.

For Fig. S4 B and C: *UAS-mitoGFP/CyO*; *park<sup>25</sup>*, *TH-GAL4/MKRS* or *park<sup>25</sup>* = sibling control or parkin mutant DA neurons, respectively.

For Fig. S4 D and E: *UAS-mitoGFP/UAS-CD8-GFP*; *park<sup>25</sup>*, *TH-GAL4/MKRS* or *park<sup>25</sup>*, *UAS-mitoGFP* = sibling control and mutant DA neurons, respectively; *Cha-GAL4*, *UAS-GFP/CyO*; *park<sup>25</sup>/MKRS* or *park<sup>25</sup>* = sibling control or parkin mutant CH neurons, respectively.

For Fig. S5: *UAS-mitoGFP/UAS-CD8GFP* or *UAS-GFP*; *park<sup>25</sup>-THGAL4/park<sup>25</sup>*, *UAS-mito-GFP* or *MKRS* = sibling control and parkin mutant DA neurons.

**Analysis of Mitochondrial Morphology.** Neural preparations stained with Mitotracker Deep Red (Mt-DR) were plated on 0.1% poly-L-lysine-coated glass cover-slips and maintained in a 5% (vol/vol) CO<sub>2</sub> incubator, at room temperature, for 2.5 h. Cultures were then fixed in 3% (wt/vol) paraformaldehyde on ice for 20 min, followed by the addition of -20 °C methanol and further incubation for 3 min on ice. Cells were then washed and incubated at 4 °C overnight with a mouse anti-GFP antibody (Molecular Probes). Following antibody incubation, cultures were washed in 1% BSA and incubated with a fluorescent secondary antibody (Molecular Probes) for 1 h at room temperature. After washing, the cover-slips were incubated for 5 min in buffer containing 4 μg/mL DAPI, then washed thoroughly, and mounted onto glass slides with Fluoromount (Sigma) for subsequent imaging by confocal microscopy. All wash and incubation solutions were prepared in Hanks Buffered Saline Solution (Media Tech). Images were processed using ImageJ software (5) and the fragmentation status of mitochondria assessed by viewing Mt-DR fluorescence in identified cell bodies. Mitochondria were determined as fused if the mitochondrion appeared continuous throughout its entire length and fragmented if mitochondria were present as multiple physically distinct entities. Mitochondrial length was determined using ImageJ software.

**Quantification of mtDNA Abundance.** Ten DA neurons were pooled by FACS into 5 μL of 10 mM Tris pH 7.9 (Sigma), 1% Triton X-100 (Sigma), and 200 μg/mL Proteinase K (Fisher). Samples were then incubated at 37 °C for 30 min, 55 °C for 30 min, 95 °C for 7.5 min, and stored at -20 °C. Quantitative PCR was performed on a Roche LightCycler 480 using standard cycling protocols. A 5' hydrolysis probe set was used to determine the Ct value of mtDNA using forward (5'-aatggagctggaacaggatg-3') and reverse (5'-aagaaatccctgctaagttagaga-3') primers and a 5' 6-carboxyfluorescein hydrolysis probe (5'-ccaccttatccgctggaattgctca-3'). The Ct value of a nuclear encoded reference gene, *α-tubulin*, was determined using Taqman assay Dm02361072\_s1. Experimental samples were normalized to *α-tubulin* Ct values, and the relative fold-change in mtDNA abundance calculated for *parkin* homozygous mutants relative to heterozygous sibling controls using the ΔΔCt method.

1. Greene JC, et al. (2003) Mitochondrial pathology and apoptotic muscle degeneration in *Drosophila parkin* mutants. *Proc Natl Acad Sci USA* 100:4078–4083.

2. Park J, et al. (2006) Mitochondrial dysfunction in *Drosophila PINK1* mutants is complemented by parkin. *Nature* 441:1157–1161.

3. Simonsen A, et al. (2008) Promoting basal levels of autophagy in the nervous system enhances longevity and oxidant resistance in adult *Drosophila*. *Autophagy* 4:176–184.
4. Deng H, Dodson MW, Huang H, Guo M (2008) The Parkinson's disease genes pink1 and parkin promote mitochondrial fission and/or inhibit fusion in *Drosophila*. *Proc Natl Acad Sci USA* 105:14503–14508.

5. Abramoff MD, Magalhaes PJ, Ram SJ (2004) Image processing with ImageJ. *Biophotonics International* 11:36–42.

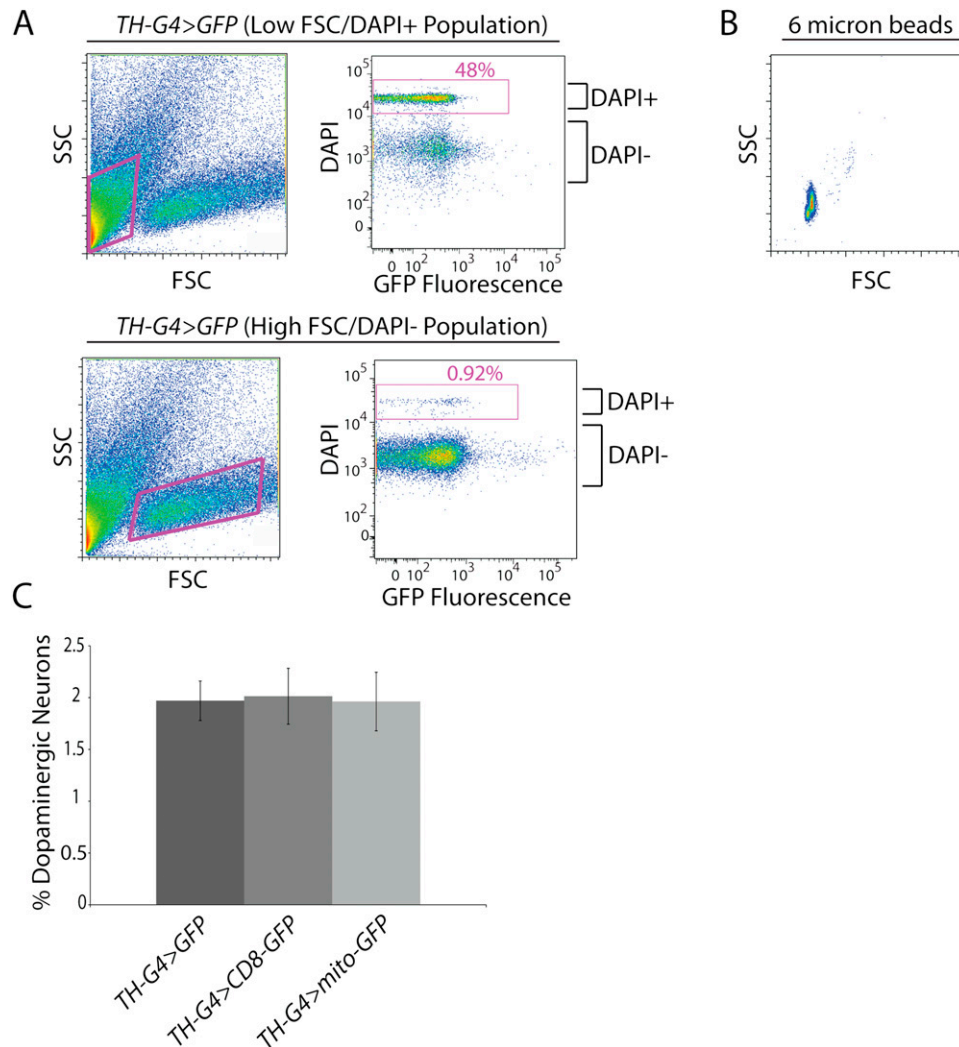


**Fig. S1.** Purification and characterization of DA neurons from the adult *Drosophila* brain. (A) A neural suspension was prepared from flies expressing GFP in DA neurons and examined by flow cytometry. A total of 123,560 particles were analyzed for forward scatter (FSC), which provides an indication of particle size, and side scatter (SSC), which provides an indication of internal cellular complexity. The purple boxes in the *Upper* and *Lower Left* define a subpopulation of 66,642 cells with low FSC values or small particle size, and a subpopulation of 20,438 cells from the same preparation with high FSC values, respectively. These two cell populations were subjected to DAPI and GFP fluorescence intensity analysis depicted in the *Upper* and *Lower Right*. The percentage of cells that fluoresce strongly with DAPI (defined by the purple boxes in the *Upper* and *Lower Right*) is indicated. (B) The FSC and SSC distribution for 6- $\mu$ m beads is shown, illustrating that the size range of the high FSC cell population in A is  $\sim$ 6  $\mu$ m, and therefore similar to the known size of the neurons of interest. (C) The proportion of DAPI<sup>-</sup>/GFP<sup>+</sup> DA neurons from flies of the indicated genotypes plotted as a percentage of the total cells observed under fluorescence gating. The number of biological replicates (*n*) and total number of cells analyzed (*N*) were as follows: *TH-G4 > GFP* (*n* = 3; *N* = 472); *TH-G4 > CD8-GFP* (*n* = 5; *N* = 1,019); *TH-G4 > mito-GFP* (*n* = 3; *N* = 255).





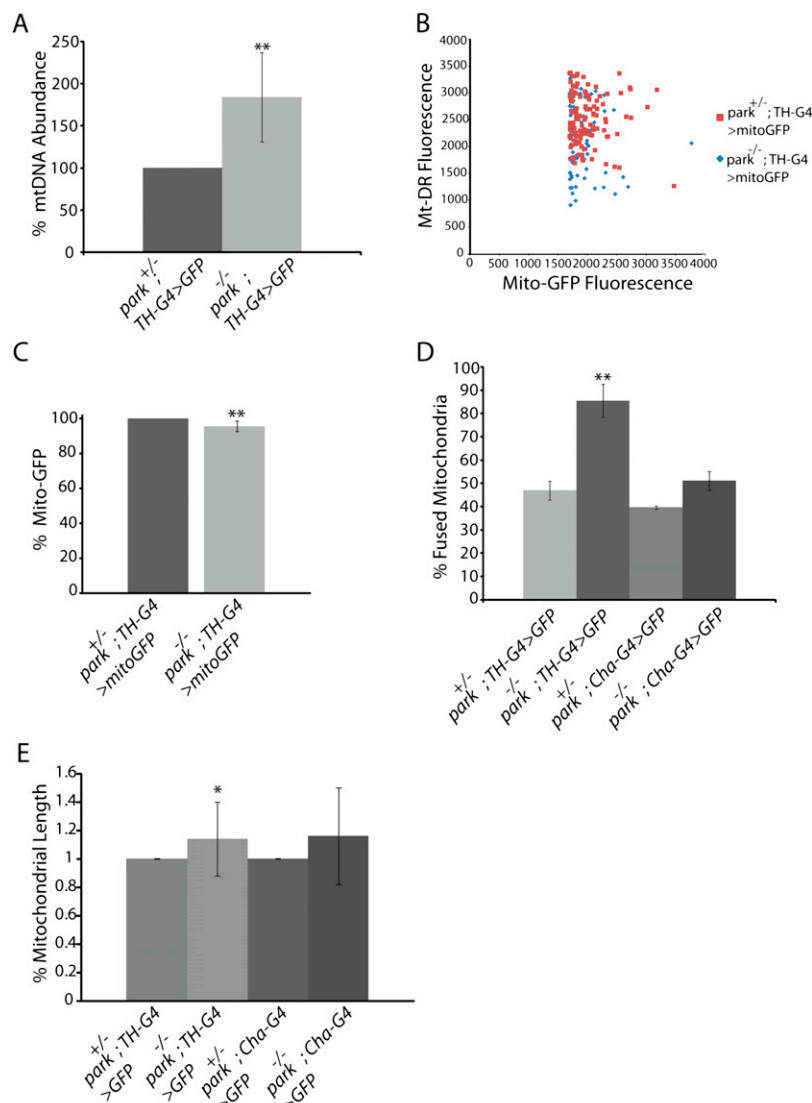


**Fig. 54.** Effect of null mutations in *parkin* on mitochondrial abundance and morphology. (A) FACS isolated DA neurons from *parkin*-null heterozygous (*park*<sup>+/-</sup>; *TH-G4* > *GFP*) and homozygous (*park*<sup>-/-</sup>; *TH-G4* > *GFP*) animals were analyzed by qPCR for mtDNA abundance relative to a reference nuclear gene. The number of biological replicates (*n*) and total number of pooled 10-cell samples analyzed (*N*) were as follows: *park*<sup>+/-</sup>; *TH-G4* > *GFP* (*n* = 3; *N* = 12); *park*<sup>-/-</sup>; *TH-G4* > *GFP* (*n* = 3; *N* = 12). Error bars represent SE. (B) Dot plot of Mt-DR fluorescence intensity relative to mito-GFP fluorescence intensity from individual dopaminergic neurons isolated from *parkin* null heterozygotes and sibling *parkin*-null homozygotes expressing mito-GFP in DA neurons (*park*<sup>+/-</sup>; *TH-G4* > *mito-GFP* and *park*<sup>-/-</sup>; *TH-G4* > *mito-GFP*, respectively). Total numbers of cells analyzed (*N*) were as follows: *park*<sup>+/-</sup>; *TH-G4* > *mito-GFP* (*N* = 113; *R*<sup>2</sup> = 0.0036); *park*<sup>-/-</sup>; *TH-G4* > *mito-GFP* (*N* = 76; *R*<sup>2</sup> = 0.013). (C) The mean relative GFP fluorescence intensity in DA neurons from *parkin*-null heterozygotes and sibling *parkin*-null homozygotes expressing mito-GFP in DA neurons (*park*<sup>+/-</sup>; *TH-G4* > *mito-GFP* and *park*<sup>-/-</sup>; *TH-G4* > *mito-GFP*, respectively). The number of biological replicates (*n*) and total number of cells analyzed (*N*) were as follows: *park*<sup>+/-</sup>; *TH-G4* > *mito-GFP* (*n* = 3; *N* = 177); *park*<sup>-/-</sup>; *TH-G4* > *mito-GFP* (*n* = 3; *N* = 116). (D) Neural cultures from *parkin*-null heterozygote controls and sibling *parkin* null homozygotes expressing GFP in DA neurons (*park*<sup>+/-</sup>; *TH-G4* > *GFP* and *park*<sup>-/-</sup>; *TH-G4* > *GFP*, respectively) or in CH neurons (*park*<sup>+/-</sup>; *Cha-G4* > *GFP* and *park*<sup>-/-</sup>; *Cha-G4* > *GFP*, respectively) were imaged by confocal microscopy. The fraction of cells exhibiting a continuous fused mitochondrion (% Fused Mitochondria) was scored relative to heterozygous controls. The number of biological replicates (*n*) and total number of cells analyzed (*N*) were as follows: *park*<sup>+/-</sup>; *TH-G4* > *GFP* (*n* = 3; *N* = 66); *park*<sup>-/-</sup>; *TH-G4* > *GFP* (*n* = 3; *N* = 62); *park*<sup>+/-</sup>; *Cha-G4* > *GFP* (*n* = 3; *N* = 48); *park*<sup>-/-</sup>; *Cha-G4* > *GFP* (*n* = 3; *N* = 47). (E) Neural cultures, as described in D, were imaged by confocal microscopy, and the length of mitochondria within these cells measured using ImageJ software (5). The fractional length of mitochondria in homozygous *parkin* mutant neurons relative to heterozygous controls is indicated (% Mitochondrial Length). The number of biological replicates (*n*) and total number of cells analyzed (*N*) were as follows: *park*<sup>+/-</sup>; *TH-G4* > *GFP* (*n* = 3; *N* = 52); *park*<sup>-/-</sup>; *TH-G4* > *GFP* (*n* = 3; *N* = 47); *park*<sup>+/-</sup>; *Cha-G4* > *GFP* (*n* = 3; *N* = 58); *park*<sup>-/-</sup>; *Cha-G4* > *GFP* (*n* = 3; *N* = 38). \**P* ≤ 0.05; \*\**P* < 0.01.

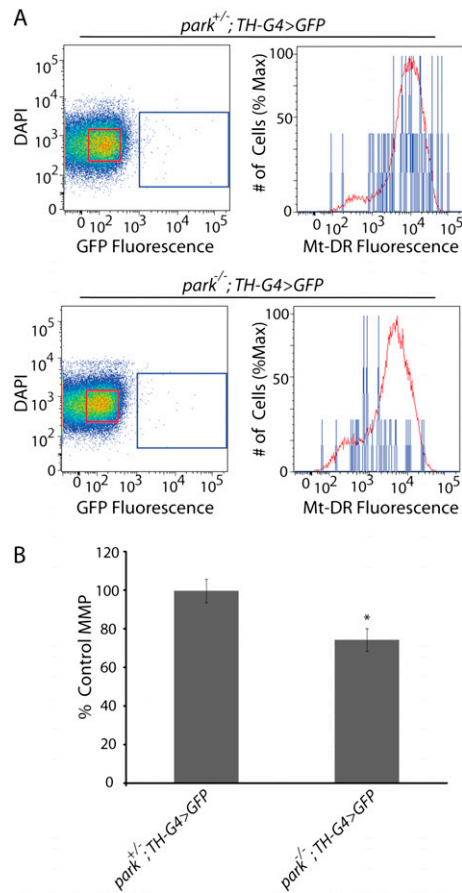


**Fig. S5.** The MMP of DA neurons relative to other neural cell types in *parkin* mutants. (A) Neural cultures from *parkin*-null heterozygotes (*park<sup>+/-</sup>; TH-G4 > GFP*) or sibling *parkin*-null homozygotes (*park<sup>-/-</sup>; TH-G4 > GFP*) expressing GFP in DA neurons were labeled with DAPI and Mt-DR and analyzed by flow cytometry. The GFP<sup>-</sup> and GFP<sup>+</sup> cell populations are demarcated within the red and blue boxes, respectively (Left). At right, Mt-DR fluorescence intensity frequency distributions from these two cell populations are shown relative to one another, with the y axis scaled as the percentage of the maximum number of cells measured for each neural cell population [# of Cells (% Max)]. (B) The mean MMP of DA neurons from the genotypes described in A expressed relative to the mean MMP of the non-GFP expressing cells in the same culture tube (% MMP). The number of biological replicates (*n*) and total number of cells analyzed (*N*) were as follows: *park<sup>+/-</sup>; TH-G4 > GFP* (*n* = 7; *N* = 330); *park<sup>-/-</sup>; TH-G4 > GFP* (*n* = 8; *N* = 444). Error bars represent SE. \**P* ≤ 0.05.